Mechanism of Photocleavage of (Coumarin-4-yl)methyl Esters

Reinhard Schmidt,*,† Daniel Geissler,‡ Volker Hagen,‡ and Jürgen Bendig§

Institute of Physical and Theoretical Chemistry, J. W. Goethe-University, Max-von-Laue-Strasse 7, D60438 Frankfurt am Main, Germany, Leibniz Institute of Molecular Pharmacology, Robert-Rössle-Strasse 10, D13125 Berlin, Germany, and Institute of Chemistry, Humboldt University, Brook-Taylor-Strasse 2, D12489 Berlin, Germany

Received: February 23, 2007; In Final Form: April 24, 2007

(Coumarin-4-yl)methyl esters (CM−A) are caged compounds that, upon excitation, release the masked biologically active acid HA and the highly fluorescent (coumarin-4-yl)methyl alcohol CM−OH very rapidly and in part with high efficiency. The results of photostationary and time-resolved investigations of 25 CM−A esters and corresponding CM−OH alcohols with varying substitution on the (coumarin-4-yl)methyl moiety and a wide variation in the structure of the acidic part have been analyzed. The initial step of the photoreaction is heterolytic ester cleavage leading to the singlet ion pair $^1[CM^+\ A^-]$ with rate constant k_1. $^1[CM^+\ A^-]$ hydrolyzes to CM−OH and HA with rate constant k_2 or recombines to ground-state CM−A with rate constant k_{rec}. $^1[CM^+\ A^-]$ is the key intermediate of the reaction. Stabilization of both CM^+ by using electron-donating substituents and A^- by increasing the acid strength leads to a strong enhancement of k_1 and simultaneously to a diminution of k_{rec}. Therefore, stabilization of the ion pair has a two-fold positive effect on the photocleavage of (coumarin-4-yl)methyl esters: increasing the rate of the initial reaction step, which might require less than 30 ps, and increasing the efficiency of product formation.

Introduction

Caged analogues of biologically active compounds receive widespread attention as temporally and spatially controlled probes of cell-based processes.[1−3] The biological activity is disabled in caged compounds by modification of an essential functionality via a photolabile chemical bond to a protecting (caging) group. Photoexcitation of the caging group induces cleavage of that bond and activates the probe.

(Coumarin-4-yl)methyl derivatives have been developed as a new class of efficient caging groups. They have been successfully applied to mask biological activity in phosphates,[4−14] carboxylates,[6,14,15] sulfates,[13] sulfonates,[13] diols,[16] and carbonyl compounds.[17] Amino and hydroxyl functionalities have also been protected via carbamate[14,18−20] or carbonate[21,22] linkers. In addition to the important applications of (coumarin-4-yl)-methyl esters (CM−A), their photochemistry is also of particular interest. CM−A compounds are among the fastest-reacting caged compounds,[6,14,23] and it is of great interest to learn how the molecular properties of their alcoholic and acidic moieties influence the rate and efficiency of the uncaging reaction. Recently, we developed Scheme 1 to describe the principal steps of the photosolvolysis of esters CM−A that lead to (coumarin-4-yl)methyl alcohol (CM−OH) and the corresponding acid HA or the acid anion A^- and H^+.[6,23]

After absorption of a photon by CM−A, relaxation to the lowest excited singlet state (S_1), $^1[CM-A]^*$, takes place. Deactivation of $^1[CM-A]^*$ occurs by fluorescence and non-radiative processes with rate constants k_{fl} and k_{nr}, respectively, and competes with heterolytic bond cleavage forming the singlet ion pair $^1[CM^+\ A^-]$ with rate constant k_1 in the initial reaction step.[6] Recombination of $^1[CM^+\ A^-]$ leads back to ground-state (S_0) CM−A with rate constant k_{rec}. Product formation is proposed to happen in two steps:[6,9] Escape from the solvent cage affords first the solvent-separated ions CM^+ and A^-. Then, the (coumarin-4-yl)methyl cation CM^+ reacts with water and undergoes a very fast deprotonation to yield the product alcohol CM−OH and H^+ in addition to the acid anion A^-. The respective first-order and pseudo-first-order rate constants are k_{esc} and k_{hyd}.

SCHEME 1

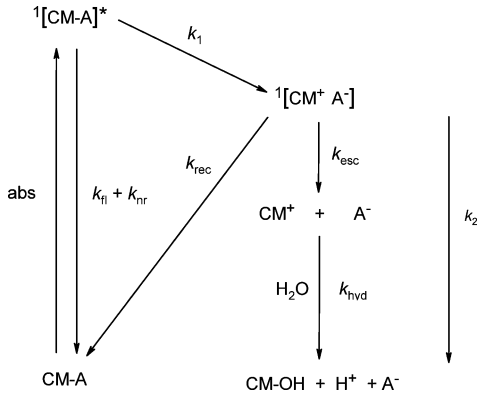

The rate constant k_1 of the initial bond cleavage is an important parameter because it influences both the rate and the efficiency of the overall uncaging reaction. Scheme 1 allows the calculation of k_1 if the fluorescence quantum yield, φ_{fl}^{OH}, and the S_1 state lifetime, τ_{OH}, of CM−OH as well as the fluorescence and photochemical quantum yields, φ_{fl}^{C} and φ_{ch}^{C}, respectively, of CM−A are known. For two different (6,7-dimethoxycoumarin-4-yl)methyl esters, we obtained the value $k_1 = 2 \times 10^{10}\ s^{-1}$, corresponding to a lifetime of the

* To whom correspondence should be addressed. E-mail: r.schmidt@chemie.uni-frankfurt.de.
† J. W. Goethe-University.
‡ Leibniz Institute of Molecular Pharmacology.
§ Humboldt University.

10.1021/jp071521c CCC: $37.00
Published on Web 06/12/2007

SCHEME 2

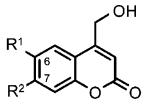

$R^1 = OCH_3$, $R^2 = H$	6-MCM-OH	$R^1 = H$, $R^2 = N(CH_3)_2$	DMACM-OH
$R^1 = H$, $R^2 = OCH_3$	7-MCM-OH	$R^1 = H$, $R^2 = N(C_2H_5)_2$	DEACM-OH
$R^1 = OCH_3$, $R^2 = OCH_3$	DMCM-OH	$R^1 = H$, $R^2 = N(CH_2CO_2H)_2$	BCMACM-OH

SCHEME 3

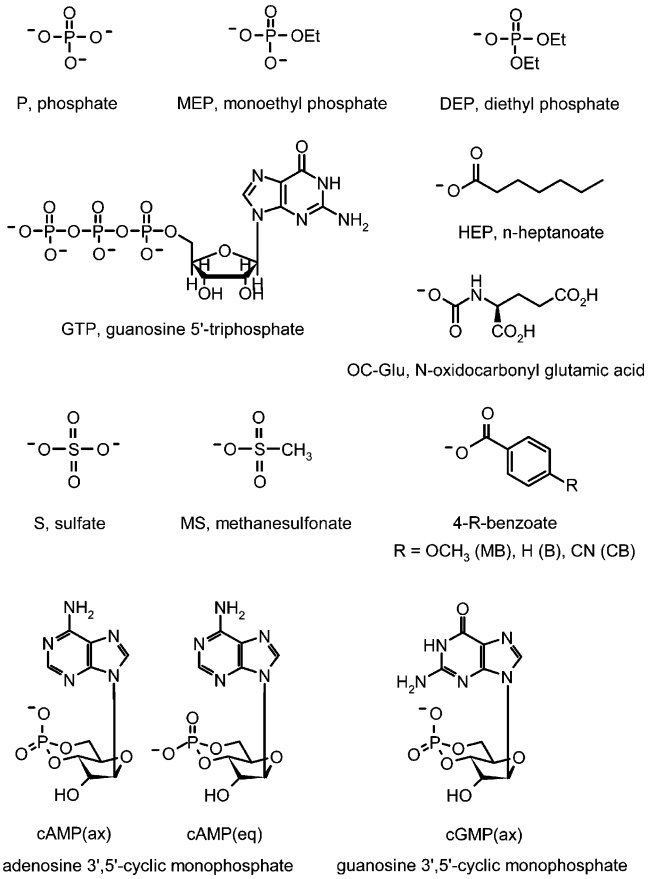

photochemically active ^{1}[CM−A]* of 50 ps. Complementary time-resolved measurements yielded significantly longer but still fast product rise times of about 0.4 ns for both caged compounds.[23]

Such quantitative stationary and time-resolved measurements of the photochemistry and fluorescence of (coumarin-4-yl)-methyl esters and the corresponding alcohols have been performed previously and are continued in the present work for a large number of esters with systematic variations of both the alcohol CM−OH and the acid HA.[6,9,10,13,14,24] This very valuable set of data is used in the present work to test the consistency of the assumed kinetics of photocleavage and to determine which properties of the esters most strongly influence the rate and efficiency of the reaction.

Scheme 2 lists the (coumarin-4-yl)methyl alcohols, and Scheme 3 shows the structures of the acid anions A^- that are products of the photosolvolysis of the investigated esters CM−A. The prefixes of the alcohols CM−OH in Scheme 2 represent the following substitutions: 6-M = 6-methoxy, 7-M = 7-methoxy, DM = 6,7-dimethoxy, DMA = 7-(dimethylamino), DEA = 7-(diethylamino), and BCMA = 7-[bis(carboxymethyl)-amino]. The structures of the investigated esters CM−A are obtained by removal of OH^- from CM−OH and addition of the resulting carbocation CM^+ to the corresponding acid anion A^-.

The structural formulas of the acid anions are drawn in such a way that, in all cases, the leftmost negatively charged O^- is the ester binding position of A^-, irrespective of eventual charge delocalization. The abbreviations used in this work for esters CM−A are additive composites of the abbreviations of the alcohols and the acid anions in Schemes 2 and 3. (ax) and (eq) indicate axial and equatorial diastereomers, respectively.

Experimental Details

The synthesis and purification of the alcohols and esters investigated has already been decribed as follows: 6-MCM−OH, 7-MCM−OH, DMCM−OH, DMACM−OH, and DEACM−OH and their cAMP(ax) and cAMP(eq) esters in ref 9; the HEP, MB, B, CB, MS, and DEP esters of 7-MCM−OH in ref 6; BCMACM−OH and its cAMP(ax) and cGMP(ax) esters in ref 14; DMACM−OH and its P ester in ref 10; the DEP, S, and MS esters of DMACM−OH in ref 13; and the OC−Glu, MEP, and GTP derivatives of DMACM−OH in ref 24. Contamination of the caged compounds with product alcohol was less than 0.1%. The compounds were stored in the dark. The methods of determining fluorescence quantum yield and photochemical quantum yield have been reported.[7,9] The photophysical and photochemical experiments were carried out under yellow light in HEPES-buffered (pH 7.2) CH_3CN/H_2O or CH_3OH/H_2O solvent mixtures or in HEPES buffer (pH 7.2) at about 23 °C. Time-resolved fluorescence rise and decay curves were recorded in a right-angle arrangement. The excitation source was an MSC 1600 N_2 laser from LTB (337 nm, 0.5 ns pulse width, 0.7 mJ maximum pulse energy). The fluorescence was excited in 1 cm × 1 cm fluorescence cells and focused through suitable interference filters by a wide-aperture collection lens on an amplified AD 110 silicon avalanche diode from Optoelectronics with a rise time of 600 ps. All signals were digitized and fed to a Tektronix TDS 620A storage oscilloscope. Variation of the laser pulse energy was achieved by use of suitable glass filters attenuating the laser beam. The apparatus function, AF(t), was obtained by irradiating a layer of MgO with N_2 laser pulses and recording the light reflected by the setup. The AF(t) curve comprises the deformation of an instantaneously decaying signal due to the finite laser pulse profile and the time response of the overall detection system. Convolutions of suitable kinetic equations $Y(t)$ with AF(t) were fitted to the experimentally recorded florescence rise and decay curves $I(t)$ by nonlinear least-squares fitting routines.[25,26]

Results and Discussion

Table 1 lists the photophysical and photochemical data of esters 7-MCM−A. Almost no changes in the wavelength, λ_{max}, or the molar absorption coefficient, ϵ_{max}, of the maximum of the long-wave absorption band are observed, despite the significant variations in the acid moiety. The comparison with the respective data for 7-MCM−OH in Table 2 demonstrates that the exchange of OH^- by A^- leads only to a sligtht red shift of 7 nm without any further change in the $S_0 \rightarrow S_1$ absorption band.

Variation of the (coumarin-4-yl)methyl substituents, however, can strongly affect the $S_0 \rightarrow S_1$ transition, as is illustrated by the data for the five alcohols CM−OH in Table 2. Both λ_{max} and ϵ_{max} vary considerably with the electron-donating ability of the substituents, i.e., with the electron density in the aromatic system. It is worth noting that, for the axial and equatorial CM−cAMP esters of each of these five alcohols, almost the same

TABLE 1: Photophysical and Photochemical Data for (7-Methoxycoumarin-4-yl)methyl Esters in 30:70 (vol/vol) CH_3CN/H_2O−HEPES Buffer (pH = 7.2)[a]

caged compound	λ_{max}[b] (nm)	ϵ_{max}[b] (M^{-1} cm^{-1})	φ_{fl}^{C}	φ_{ch}^{C}	k_1 (10^9 s^{-1})	τ_C (ns)	φ_1	f_2	k_{rec}/k_2
7-MCM−HEP	324	13500	0.37	0.0043	0.32	0.98	0.31	0.014	72
7-MCM−MB	324	13600	0.42	0.0045	0.20	1.1	0.22	0.020	48
7-MCM−B	324	13000	0.43	0.0052	0.18	1.1	0.20	0.026	38
7-MCM−CB	324	13700	0.08	0.0064	4.0	0.21	0.85	0.008	132
7-MCM−MS	325	13000	0.007	0.081	52	0.02	0.99	0.082	11
7-MCM−DEP	324	13900	0.052	0.037	6.6	0.14	0.90	0.041	23

[a] Data from ref 6. [b] Absorption maximum of $S_0 \rightarrow S_1$ transition.

TABLE 2: Photophysical Data for Differently Substituted (Coumarin-4-yl)methyl Alcohols in CH_3OH/H_2O−HEPES Buffer (pH = 7.2)

alcohol	λ_{max}[a] (nm)	ϵ_{max}[a] (M^{-1} cm^{-1})	τ_{OH}[b] (ns)	φ_{fl}^{OH}[b]	k_{fl} (10^8 s^{-1})	k_{nr} (10^8 s^{-1})
6-MCM−OH[c]	337	4800	2.67	0.16	0.60	3.15
7-MCM−OH[c]	317	13300	3.50	0.65	1.86	1.00
DMCM−OH[c]	341	11700	4.90	0.59	1.20	0.84
DMACM−OH[d]	378	17800	2.10[e]	0.21	1.00	3.76
DEACM−OH[d]	387	20900	0.91[e]	0.082	0.90	10.1

[a] Absorption maximum of $S_0 \rightarrow S_1$ transition. [b] Unlabeled τ_{OH} and φ_{fl}^{OH} data are from ref 9. [c] 20:80 (vol/vol). [d] 50:50 (vol/vol). [e] This work.

red shift of λ_{max} and the same increase of ϵ_{max} are observed (see Table 3). The average red shift between the ester and the corresponding alcohol is, at 10 nm, similarly small as in the case of the 7-MCM esters in Table 1.

Variation of the electron density of the aromatic systems influences λ_{max} and ϵ_{max} of the alcohol CM−OH and the corresponding ester CM−A in much the same way. Thus, the $S_0 \rightarrow S_1$ absorption changes only slightly between CM−OH and CM−A. The unchanged values of ϵ_{max} indicate that the fluorescence rate constants, k_{fl}, are the same for the alcohol and the corresponding ester. In fact, the fluorescence quantum yields, φ_{fl}^{C}, and lifetimes, τ_C, of the esters CM−A are of similar size as the respective φ_{fl}^{OH} and τ_{OH} values for the corresponding alcohols CM−OH for esters CM−A with very low photochemical quantum yields, φ_{ch}^{C}, as will be shown later. This indicates that the nonradiative deactivation $S_1 \rightarrow S_0$ occurs in the ester CM−A and the corresponding alcohol CM−OH at the same rate. Thus, for corresponding CM−OH/CM−A pairs, we assume $k_{fl} = k_{fl}^{OH} = k_{fl}^{C}$ and $k_{nr} = k_{nr}^{OH} = k_{nr}^{C}$.

The rate constants of the physical and chemical processes given in Scheme 1 are related to the experimentally accessible quantities φ_{fl}^{OH}, τ_{OH}, φ_{fl}^{C}, φ_{ch}^{C}, and τ_C by eqs 1−5

$$\varphi_{fl}^{OH} = k_{fl}/(k_{fl} + k_{nr}) \quad (1)$$

$$\tau_{OH} = 1/(k_{fl} + k_{nr}) \quad (2)$$

$$\varphi_{fl}^{C} = k_{fl}/(k_{fl} + k_{nr} + k_1) \quad (3)$$

$$\tau_C = 1/(k_{fl} + k_{nr} + k_1) \quad (4)$$

$$\varphi_{ch}^{C} = [k_1/(k_{fl} + k_{nr} + k_1)] \times [k_2/(k_{rec} + k_2)] = \varphi_1 f_2 \quad (5)$$

where φ_1 is the quantum yield of ion-pair formation and f_2 is the efficiency of CM−OH formation in the decay of $^1[CM^+ A^-]$. Our experiments allow no distinction between the two reaction steps on the way from $^1[CM^+ A^-]$ to CM−OH given in Scheme 1. Therefore, we combine the two together into a single step with rate constant $k_2 \approx k_{esc}k_{hyd}/(k_{esc} + k_{hyd})$, where the smaller of the two rate constants mainly determines the value of k_2.[23]

Table 1 also presents the fluorescence and photochemical quantum yields, φ_{fl}^{C} and φ_{ch}^{C}, respectively, of the 7-MCM−A esters as determined in a buffered CH_3CN/H_2O (30:70 vol/vol) mixture. The esters with large φ_{fl}^{C} values of about 0.4 have only very small values of φ_{ch}^{C}. Obviously, the photochemical path contributes only a small amount to the overall deactivation of the S_1 excited 7-MCM−A esters in those cases. Therefore, we expect fluorescence quantum yields, φ_{fl}^{OH}, of similar size for these esters and for 7-MCM−OH. Actually, for 7-MCM−OH, in addition to $\tau_{OH} = 1.43$ ns, we determined $\varphi_{fl}^{OH} = 0.54$ in that solvent mixture. The deviation of this slightly larger-than-expected value of φ_{fl}^{OH} still lies within the limits of our simplifying assumptions about the radiative and nonradiative $S_1 \rightarrow S_0$ deactivation of CM−OH and corresponding CM−A. Using the two results, we calculate $k_{fl} = 3.78 \times 10^8$ s^{-1} and $k_{nr} = 3.22 \times 10^8$ s^{-1} for 7-MCM−OH in 30:70 (vol/vol) CH_3CN/HEPES buffer. Assuming that these values are also valid for the 7-MCM−A esters and using the previously published experimental values of φ_{fl}^{C} and φ_{ch}^{C} in Table 1, we obtain via eqs 3 and 4 the rate constants k_1 and the S_1 state lifetimes τ_C listed in Table 1. According to these new results, we see a strongly graduated rate of photoheterolysis. The reaction is very fast for 7-MCM−MS and fast for 7-MCM−CB and 7-MCM−DEP. The rest of the esters in Table 1 react more slowly.

Our previously published φ_{fl}^{C} and φ_{ch}^{C} data for the axial and equatorial CM−cAMP esters in Table 3 have also not been evaluated in this way before.[9] Using the k_{fl} and k_{nr} values of the corresponding (coumarin-4-yl)methyl alcohols in Table 2, we obtain the values of k_1 and τ_C listed in Table 3. A quick inspection of these new results reveals that all CM−cAMP esters of the five alcohols react rapidly. However, particularly rapid initial reactions should be noted for the cAMP esters of DMACM−OH and DEACM−OH.

Table 4 collects the new fluorescence and photochemical quantum yields of two esters of BCMACM−OH and seven esters of DMACM−OH. Figure 1 shows the rise and decay of the fluorescence, $I(t)$, of BCMACM−OH measured after laser pulse excitation in 5:95 CH_3CN/H_2O (HEPES buffer, pH = 7.2), as well as the fit of the convolution of $Y(t) = A \exp(-t/\tau_{OH})$ with the apparatus function $AF(t)$ to $I(t)$. The fluorescence lifetime $\tau_{OH} = 1.59$ ns results as the average of several measurements. Results of an analogous experiment with DMACM−OH, for which a mean value of $\tau_{OH} = 1.15$ ns is obtained, are shown in Figure 2. The corresponding fluorescence quantum yields, $\varphi_{fl}^{OH} = 0.17$ (BCMACM−OH) and $\varphi_{fl}^{OH} = 0.13$ (DMACM−OH), were measured in the same solvent mixture. Combining the φ_{fl}^{C} and φ_{ch}^{C} data with these results leads to the values of k_1 and τ_C listed in Table 4.

Again, very different rates of photoheterolysis are found. The calculated S_1 state lifetimes, τ_C, of the OC−Glu, P, MEP, and GTP esters of DMACM−OH are, at about 1 ns, rather long. Because short-lived intermediates have to be passed on the way from the singlet excited CM−A to CM−OH, the rise time, τ_A, of the product alcohol should be significantly larger than τ_C.

TABLE 3: Photophysical and Photochemical Data for Cyclic Adenosine Monophosphate Esters of Differently Substituted (Coumarin-4-yl)methyl Alcohols in CH_3OH/H_2O−HEPES Buffer (pH = 7.2)[a]

caged compound	λ_{max}[b] (nm)	ϵ_{max}[b] (M^{-1} cm^{-1})	φ_{fl}^C	φ_{ch}^C	k_1 (10^9 s^{-1})	τ_C (ns)	φ_1	f_2	k_{rec}/k_2
6-MCM−cAMP(ax)[c]	346	4500	0.008	0.03	7.1	0.13	0.95	0.032	31
7-MCM−cAMP(ax)[c]	328	13200	0.030	0.13	5.9	0.16	0.95	0.14	6.3
DMCM−cAMP(ax)[c]	349	11000	0.021	0.04	5.5	0.17	0.96	0.041	23
DMACM−cAMP(ax)[d]	394	17200	0.0085	0.28	11	0.09	0.96	0.29	2.4
DEACM−cAMP(ax)[d]	402	18600	0.0055	0.21	15	0.06	0.93	0.23	3.4
6-MCM−cAMP(eq)[c]	345	4200	0.0085	0.02	6.7	0.14	0.95	0.021	46
7-MCM−cAMP(eq)[c]	325	13300	0.040	0.07	4.4	0.22	0.94	0.075	12
DMCM−cAMP(eq)[c]	346	11500	0.023	0.04	5.0	0.19	0.96	0.042	23
DMACM−cAMP(eq)[d]	387	16100	0.007	0.26	14	0.07	0.97	0.27	2.7
DEACM−cAMP(eq)[d]	396	20200	0.006	0.23	14	0.07	0.93	0.25	3.0

[a] Data are from ref 9. [b] Absorption maximum of $S_0 \rightarrow S_1$ transition. [c] 20:80 (vol/vol). [d] 50:50 (vol/vol).

TABLE 4: Photophysical and Photochemical Data for (Coumarin-4-yl)methyl Esters in CH_3CN/H_2O−HEPES Buffer Mixtures of Various Concentrations[a−c] (pH = 7.2) As Determined in the Present Work

caged compound	φ_{fl}^C	φ_{ch}^C	k_1 (10^9 s^{-1})	τ_C (ns)	τ_M (ns)	τ_{OH} or τ_C (ns)	φ_1	f_2	k_{rec}/k_2
BCMACM−cAMP[d]	0.007[a,e]	0.26[a,f]	15[g]	0.07[g]	0.36[g,i]	1.97[e,i] (OH)	0.96[f]	0.27[g]	2.7[h]
BCMACM−cGMP[d]	0.008[a,e]	0.25[a,f]	13[g]	0.07[g]	0.21[g,i]	1.66[e,i] (OH)	0.95[f]	0.26[g]	2.8[h]
DMACM−DEP	0.006[a,e]	0.36[a,f]	18[g]	0.05[g]	≤0.2[i,j]	1.03[e,i] (OH)	0.95[f]	0.38[g]	1.65[h]
DMACM−S	0.011[a,e]	0.46[c,f]	9.5[g]	0.10[g]	≤0.2[i,j]	1.08[e,i] (OH)	0.92[f]	0.50[g]	1.0[h]
DMACM−MS	0.002[b,e]	0.79[b,f]	56[g]	0.02[g]			0.98[f]	0.80[g]	0.25[k]
DMACMOC−Glu	0.10[a,f]	0.02[c,h]	0.26[k]	0.88[h]		1.08[e,i] (C)	0.23[g]	0.09[k]	11[k]
DMACM−P	0.14[a,f]	0.03[c,h]	−0.06[m]	1.23[h]		1.26[e,i] (C)			
DMACM−MEP	0.10[a,f]	0.03[c,h]	0.26[k]	0.88[h]		0.96[e,i] (C)	0.23[g]	0.13[k]	7[k]
DMACM−GTP	0.12[a,f]	0.05[c,e]	0.07[k]	1.06[h]		1.20[e,i] (C)	0.08[k]	0.65[k]	0.5[l]

[a−c] CH_3CN/H_2O: (vol/vol): *a*, 5:95; *b*, 20:80; *c*, 0:100. [d] (ax). [e−h] Average uncertainties: *e*, ±15%; *f*, ±10%; *g*, ±30%; *h*, ±20%. [i] Single-pulse experiment. [j] Limit of accuracy. [k] Factor of 2. [l] Factor of 6. [m] Meaningless negative value of k_1 is caused by the fact that $\varphi_{fl}^C > \varphi_{fl}^{OH}$. $\varphi_{fl}^C - \varphi_{fl}^{OH} = 0.01$ lies in the mutual error limits of φ_{fl}^C and φ_{fl}^{OH} (5%).

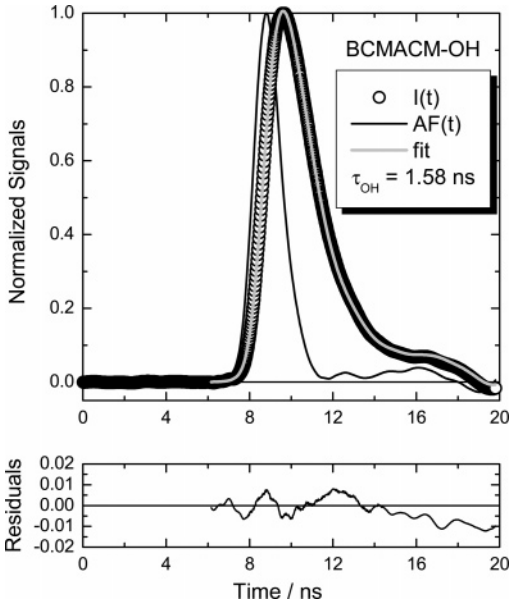

Figure 1. Normalized fluorescence decay of BCMACM−OH in 5:95 (vol/vol) CH_3CN/H_2O (HEPES buffer); 496 nm interference filter. Fit is a convolution of AF(t) with $Y(t) = A \exp(-t/\tau_{OH})$.

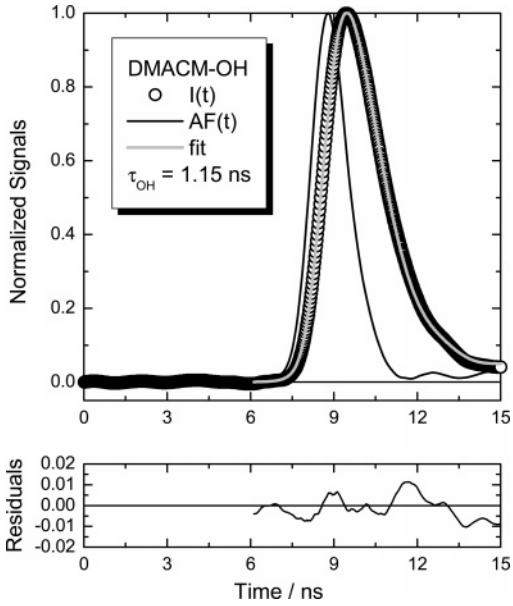

Figure 2. Normalized fluorescence decay of DMACM−OH in 5:95 (vol/vol) CH_3CN/H_2O (HEPES buffer); 496 nm interference filter. Fit is a convolution of AF(t) with $Y(t) = A \exp(-t/\tau_{OH})$.

Therefore, formation of DMACM−OH during the excitation pulse, which has a half-width of 0.5 ns, is not expected. However, the situation could be different for the (coumarin-4-yl)methyl esters in Table 4, for which values of $0.02 \leq \tau_C \leq 0.1$ ns were obtained. In fact, it has recently been demonstrated for DMCM−DEP and DMCM−S by time-resolved fluorescence measurements that the product DMCM−OH is formed *and* excited during the same single excitation pulse with rise time $\tau_A \approx 0.4$ ns.[23] Because Table 4 also includes data on very rapidly reacting esters, the verification of the evaluation of the photostationary data by eqs 3 and 4 according to Scheme 1 is possible by means of a complementary time-resolved fluorescence study. We therefore measured fluorescence rise and decay curves, $I(t)$, upon single-pulse excitation for most of the esters in Table 4.

The question of whether the product alcohol is already formed during the laser pulse can be answered by analysis of the $I(t)$ curves. It is important that the ester and alcohol absorb and emit via the same (coumarin-4-yl)methyl chromophore, i.e., in the same spectral region. If the product alcohol is already formed during the laser pulse used for excitation of the ester, its fluorescence can be excited by a second photon of the same laser pulse, thus adding to the direct fluorescence of the ester to yield the overall fluorescence rise and decay signal $I(t)$. Whereas the concentration of the ester is almost constant during

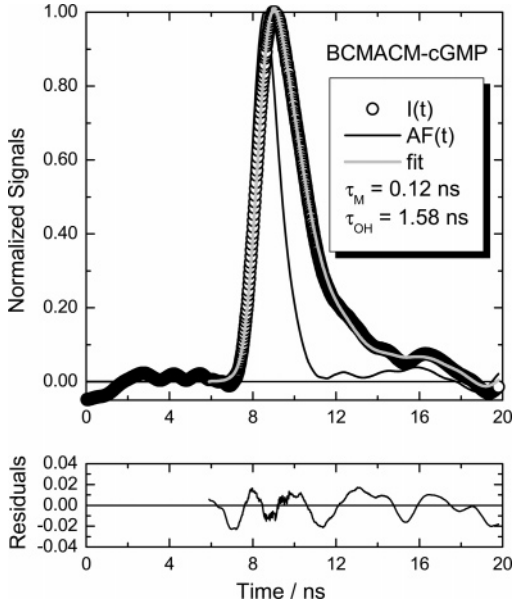

Figure 3. Normalized fluorescence decay of BCMACM−cGMP(ax) in 5:95 (vol/vol) CH_3CN/H_2O (HEPES buffer); 496 nm interference filter. Fit is a convolution of AF(t) with eq 6.

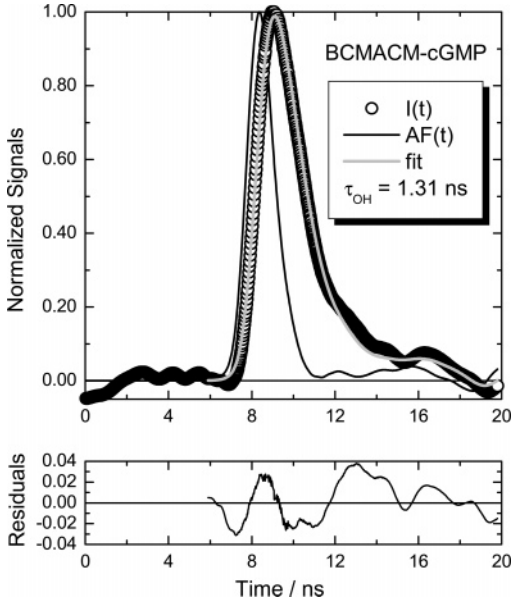

Figure 4. Normalized fluorescence decay of BCMACM−cGMP(ax) in 5:95 (vol/vol) CH_3CN/H_2O (HEPES buffer); 496 nm interference filter. Fit is a convolution of AF(t) with $Y(t) = A \exp(-t/\tau_{OH})$.

the low-energy pulse excitation, the concentration of the product alcohol follows a sigmoidal rise function whose width and location on the time scale depend on the laser pulse width and τ_A. For the very rapidly reacting esters, $\varphi_{fl}^{OH} \gg \varphi_{fl}^{C}$. In these cases, the contribution of the ester fluorescence to the overall fluorescence signal dominates only in the very early part because $\tau_C < \tau_A$. At later times, the fluorescence of the just-formed alcohol prevails, because $\tau_C < \tau_{OH}$ and $\varphi_{fl}^{OH} \gg \varphi_{fl}^{C}$. We have recently shown that, in such a case, where monophotonic and biphotonic fluorescence signals contribute, the time course of the overall signal $I(t)$ can be fitted by the convolution of the single-photon apparatus function AF(t) with the simplified biexponential kinetics $Y(t)$ of eq 6.[23]

$$Y(t) = A \exp(-t/\tau_M) + B \exp(-t/\tau_{OH}) \qquad (6)$$

Here, the individual time constants τ_C and τ_A have been replaced by a common time constant τ_M, which is interpreted roughly as the mean value of the two. Convolutions of AF(t) with eq 6 with four variables (A, B, τ_M, τ_{OH}) could well be fitted to the experimental fluorescence curves $I(t)$. The quality of the fits obtained is very good, as illustrated in Figure 3, although the $I(t)$ curves are somewhat noisy results of being single-laser-pulse experiments.

For comparison, Figure 4 displays the fit of the convolution of AF(t) with $Y(t) = A \exp(-t/\tau_{OH})$ to the experimental rise and decay curve $I(t)$ of Figure 3, which results in $\tau_{OH} = 1.3$ ns. The description of the experiment is significantly worse. This can also be seen by the larger residuals and by the 3-times-larger χ^2 value of the monoexponential fit.

The comparison of the rise and decay curves of Figures 3 and 1 shows a clearly steeper rise of the fluorescence for BCMACM−cGMP than for BCMACM−OH. The steeper rise can qualitatively be explained by the rapid increase of the product alcohol absorbance occurring already during the exciting laser pulse in the first case, whereas in the latter case, no increase of alcohol absorbance takes place. This leads to a biphotonic origin of the BCMACM−OH fluorescence in the case of the photolysis of the BCMACM−cGMP ester. The time constant $\tau_{OH} = 1.58$ ns obtained for the BCMACM−cGMP experiment of Figure 3 agrees with the fluorescence lifetime $\tau_{OH} = 1.59$ ns of BCMACM−OH. Averaging over the individual experiments leads to the τ_{OH} and τ_M values reported in Table 4. We note the very good agreement between the average time constants, τ_{OH}, of the first four CM−A esters and the fluorescence lifetimes, τ_{OH}, of the corresponding CM−OH alcohols (for DMACM−OH, $\tau_{OH} = 1.15$ ns). Only for BCMACM−cAMP is the fit value too large by 25%. These results verify that the product alcohol is actually formed and excited by a second photon of the same laser pulse for the very rapidly reacting esters.

The second time constant, τ_M, obtained in these experiments provides information about the rate of product formation. Considering τ_M as the mean value of τ_C and τ_A, very short rise times for BCMACM−OH of 0.4−0.7 ns and for DMACM−OH of $\leq$0.4 ns are estimated, which fit into the width of the exciting laser pulse. Therefore, the evaluations of the time-resolved and photostationary experiments are consistent.

Figure 5 illustrates the fluorescence rise and decay recorded for DMACM−MEP as an example of the relatively slowly reacting esters. None of the fluorescence curves, including that of DMACM−MEP, could be fitted by a convolution of AF(t) with $Y(t)$ in the form of eq 6. Different kinetics have to be used. A comparison of Figures 5 and 2 shows almost identical fluorescence increases for DMACM−MEP and DMACM−OH. Obviously, the very fast component of the biphotonic contribution to the overall fluorescence seen with BCMACM−cGMP in Figure 3 is missing. In other words, the rise of the product alcohol absorbance is so slow that excitation of DMACM−OH by a second photon of the photolysis pulse is impossible. Therefore, Figure 5 simply illustrates the rise and decay of the monophotonic ester fluorescence, which follows first-order kinetics. The good fit to $I(t)$ of the convolution of AF(t) with a monoexponential decay function yields the lifetime $\tau_C = 0.99$ ns for S_1 excited DMACM−MEP. However, no information about the rate of product alcohol formation is gained in the experiments with the relatively slow esters. The lower four entries of the last column of time constants in Table 4 represent the average experimental S_1 state lifetimes, τ_C, of the relatively slowly reacting DMACM esters. A good agreement between these values and the S_1 state lifetime of DMACM−OH ($\tau_{OH} = 1.15$ ns) is found, confirming the above assumption that $k_{fl} =$

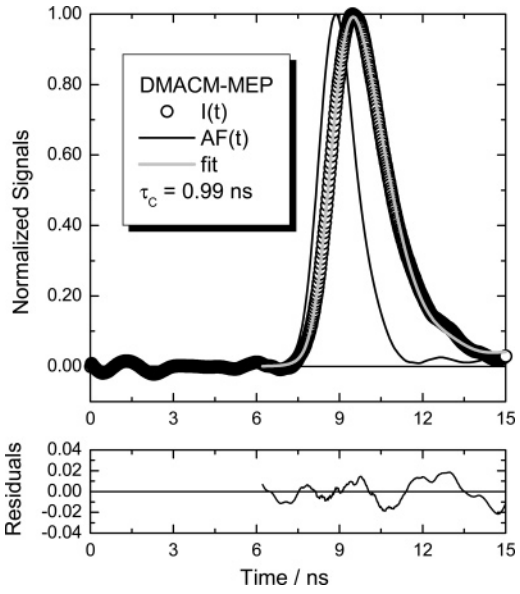

Figure 5. Normalized fluorescence decay of DMACM−MEP in 5:95 (vol/vol) CH_3CN/H_2O (HEPES buffer); 496 nm interference filter. Fit is a convolution of AF(t) with $Y(t) = A \exp(-t/\tau_C)$.

$k_{fl}^{OH} = k_{fl}^{C}$ and $k_{nr} = k_{nr}^{OH} = k_{nr}^{C}$ for corresponding CM−OH/CM−A pairs. In fact, we calculate from the experimental φ_{fl}^{C} and τ_C values of these four DMACM esters average values of $k_{fl}^{C} = 1.0 \times 10^8\ s^{-1}$ and $k_{nr}^{C} = 8.0 \times 10^8\ s^{-1}$ in accordance with the results of $k_{fl}^{OH} = 1.1 \times 10^8\ s^{-1}$ and $k_{nr}^{OH} = 7.6 \times 10^8\ s^{-1}$ found with φ_{fl}^{OH} and τ_{OH} of DMACM−OH. Furthermore, we note that the calculated S_1 state lifetimes τ_C agree rather well with the respective experimental τ_C data. We conclude that the photostationary and complementary time-resolved studies lead to a completely consistent picture. Therefore, we can rely on the k_1 values listed in Tables 1, 3, and 4.

Insertion of electron-donating substituents into the coumarin-4-yl system leads to strong bathochromic shift of the $S_0 \rightarrow S_1$ absorption of CM−OH and CM−A as well. The effect is significantly larger at the 6- than at the 7-position, which has been explained by a larger difference of MO coefficients of the HOMO and LUMO at the 6-position.[9] The increase of electron density of the coumarin-4-yl system causes the red shift of the $S_0 \rightarrow S_1$ $\pi\pi^*$ absorption band. Inspection of the data for the CM−cAMP esters in Table 3 indicates that the pronounced red shift of this absorption is accompanied by a strong increase of k_1 illustrated by the linear correlation of log(k_1) with the wavenumber, ν_{max}, of the maximum of the $S_0 \rightarrow S_1$ absorption shown in Figure 6.

The increase of electron density stabilizes the carbocation CM^+ that is a component of the primary intermediate of photocleavage, the singlet ion pair $^1[CM^+\ A^-]$. Thus, we conclude that the stabilization of CM^+ causes an increase of the rate constant k_1.

Tables 1 and 4 list rate constants k_1 of 7-MCM−A and DMACM−A esters with a wide variation of the acidic component. k_1 reaches maximum values when the strong methansulfonic acid is released, whereas smaller values of k_1 result for weak acids, revealing that the acid strength is an important factor affecting the rate of photocleavage of (coumarin-4-yl)methyl esters. Table 5 lists pK_a values of the acids being released in the photolysis of DMACM−A and 7-MCM−A. Glutamic acid is bound in DMACMOC−Glu as carbamate. Thus, the pK_a relevant for glutamate release is that of carbamic acid given in Table 5. Figure 7 shows the linear free energy relationship (LFER) of log(k_1) with pK_a.

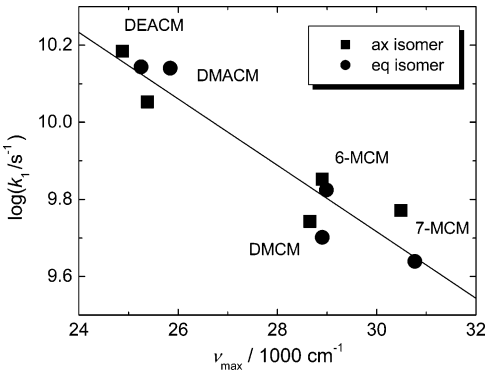

Figure 6. Correlation of log(k_1) with the wavenumber, ν_{max}, of the maximum of the $S_0 \rightarrow S_1$ absorption band of CM−cAMP esters of differently substituted (coumarin-4-yl)methyl alcohols in CH_3OH/HEPES. The straight line with slope = −0.086 per 1000 cm^{-1} and intercept = 12.3 results from a linear fit to the respective data in Table 3.

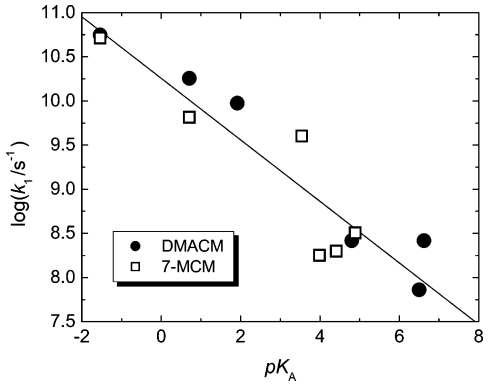

Figure 7. Linear free energy relation between log(k_1) and the pK_a values of the acids released during the photolysis of DMACM and 7-MCM esters in CH_3CN/HEPES. The straight line with slope = −0.35 and intercept = 10.26 results from a linear fit to the respective data in Tables 1, 4, and 5.

TABLE 5: pK_a Values of Acids Released in the Photolysis of the 7-MCM−A and DMACM−A Esters in Tables 1 and 4

acid	pK_a	acid	pK_a
n-heptanoic	4.89[a]	methanesulfonic	−1.54[a]
4-methoxybenzoic	4.41[a]	sulfuric[f]	1.92[c]
benzoic	3.99[a]	diethyl phosphoric	0.71[a]
4-cyanobenzoic	3.54[a]	monoethyl phosphoric[f]	6.62[d]
carbamic	4.8[b]	phosphoric[f]	7.21[c]
		guanosine 5-triphosphoric	6.5[e]

[a] Reference 6. [b] Reference 27. [c] Reference 28. [d] Reference 29. [e] Reference 30. [f] Second step.

The straight line drawn in Figure 7 is the result of a linear fit to all of the data and describes the experimental values rather well. However, most of the 7-MCM−A data are below the line, whereas the DMACM−A data deviate from the line more in the direction toward larger values. This difference is caused by the different electron-donating abilities of the (coumarin-4-yl)-methyl substituents, which leads to log(k_1) values for the DMACM−cAMP esters in CH_3CN/HEPES buffer that are 0.4 units larger than the corresponding data for the 7-MCM−cAMP esters (see Figure 6). It appears that the strength of the photoreleased acid influences the rate constant k_1 independent of the (coumarin-4-yl) substituent, i.e., independent of the stabilization of the carbocation. With decreasing pK_a, and hence with decreasing basicity of the acid anion, a strong increase of log(k_1) results. Thus, it is the stabilization of the acid anion A^-, the second component of the singlet ion pair $^1[CM^+\ A^-]$,

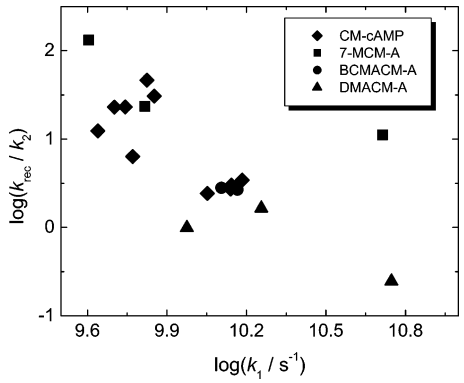

Figure 8. Correlation of $\log(k_{rec}/k_2)$ with $\log(k_1)$ for CM−A esters with quantum yields of ion-pair formation $\varphi_1 > 0.85$.

that causes the augmentation of the rate constant k_1 by 1 order of magnitude when the pK_a is lowered by three units.

The fate of the ion pair $^1[CM^+\ A^-]$ is recombination to the ground-state ester CM−A with rate constant k_{rec} or reaction to the alcohol CM−OH and acid HA by cage escape and hydrolysis with overall rate constant k_2. Unfortunately, neither of the two rate constants can be evaluated from our data. However, the ratio $k_{rec}/k_2 = 1/f_2 - 1$ is accessible via the efficiency $f_2 = \varphi_{ch}^C/\varphi_1$. The recombination reaction should depend on the stabilization of both components CM^+ and A^-, similar to ion-pair formation but with opposite sign. It is expected that k_{rec} decreases with increasing stability of both CM^+ and A^- and thus with increasing rate constant k_1. If cage escape is the rate-determining step of the second reaction, no significant effect of ion stabilization on k_2 is expected, and a clear inverse correlation of k_{rec}/k_2 with k_1 should result. If hydrolysis is rate-determining, then stabilization of CM^+ should lead to smaller rate constants k_2. However, because the variation of the acid strength influences k_1 more strongly than the electronic stabilization of CM^+ (compare Figures 6 and 7), CM^+ and A^- stabilization will, in any case, more strongly affect k_{rec} than k_2. Thus, in the latter case, we also expect an inverse correlation of k_{rec}/k_2 with k_1. The uncertainty of f_2 increases dramatically with decreasing value of φ_1. Therefore, we used k_{rec}/k_2 data for only those esters for which $\varphi_1 > 0.85$. Figure 8 displays the still-large data set in a plot of $\log(k_{rec}/k_2)$ versus $\log(k_1)$.

With the exception of 7-MCM−MS, a roughly linear correlation between $\log(k_{rec}/k_2)$ and $\log(k_1)$ with negative slope is found, indicating that the factors that accelerate the heterolytic bond cleavage retard the ion-recombination reaction. This, in turn, favors an increase in the efficiency f_2 of the competing product formation.

Conclusions

The conclusion of our quantitative investigation of the primary step of the photocleavage of (coumarin-4-yl)methyl esters is rather simple but reasonable. A significant weakening of the CM−A ester bond takes place upon excitation of the (coumarin-4-yl)methyl ester to S_1 if both components of the singlet ion pair $^1[CM^+\ A^-]$ are stabilized. Stabilization of the carbocation CM^+ is achieved by use of substituents with strong electron-donating abilities; stabilization of acid anions A^- is achieved by selection of anions with low basicities and large pK_b values. This explains why both (coumarin-4-yl)methyl alcohols (leaving group OH^-, $pK_b = -1.7$) and alkyl ethers (leaving group ^-OR) are resistant to photoheterolysis. Furthermore, the factors that accelerate heterolytic bond cleavage retard the ion-recombination reaction. Therefore, stabilization of the ion pair $^1[CM^+\ A^-]$ has a two-fold positive effect on the photocleavage of (coumarin-4-yl)methyl esters: increasing (i) the rate of the initial reaction step and (ii) the efficiency of product formation.

Acknowledgment. Financial support from the Adolf Messer Stiftung and the Fonds der Chemischen Industrie is gratefully acknowledged.

References and Notes

(1) Mariott, G., Ed. Caged Compounds. In *Methods in Enzymology*; Academic Press: New York, 1998; Vol. 291.

(2) Pelliccioli, A. P.; Wirz, J. *Photochem. Photobiol. Sci*. **2000**, *1*, 441−458.

(3) Goeldner, M.; Givens, R. S., Eds. *Dynamic Studies in Biology: Phototriggers, Photoswitches and Caged Biomolecules*; Wiley-VCH: Weinheim, Germany, 2005.

(4) Givens, R. S.; Matuszewski, B. *J. Am. Chem. Soc*. **1984**, *106*, 6860−6861.

(5) Furuta, T.; Torigai, H.; Sugimoto, M.; Iwamura, M. *J. Org. Chem.* **1995**, *60*, 3953−3956.

(6) Schade, B.; Hagen, V.; Schmidt, R.; Herbrich, R.; Krause, E.; Eckardt, T.; Bendig, J. *J. Org. Chem*. **1999**, *64*, 9109−9117.

(7) Hagen V.; Bendig, J.; Frings, S.; Wiesner, B.; Schade, B.; Helm, S.; Lorenz, D.; Kaupp, U. B. *J. Photochem. Photobiol. B: Biol*. **1999**, *53*, 91−102.

(8) Hagen, V.; Bendig, J.; Frings, S.; Eckardt, T.; Helm, S.; Reuter, D.; Kaupp, U. B. *Angew. Chem., Int. Ed.* **2001**, *40*, 1045−1048.

(9) Eckardt, T.; Hagen, V.; Schade, B.; Schmidt, R.; Schweitzer, C.; Bendig, J. *J. Org. Chem.* **2002**, *67*, 703−710.

(10) Geissler, D.; Kresse, W.; Wiesner, B.; Bendig, J.; Kettenmann, H.; Hagen, V. *ChemBioChem* **2003**, *4*, 162−170.

(11) Hagen, V.; Frings, S.; Wiesner, B.; Helm, S.; Kaupp, U. B.; Bendig, J. *ChemBioChem* **2003**, *4*, 434−442.

(12) Furuta, T.; Takeuchi, H.; Isozaki, M.; Takahashi, Y.; Kanehara, M.; Sugimoto, M.; Watanabe, T.; Noguchi, K.; Dore, T. M.; Kurahashi, T.; Iwamura, M.; Tsien, R. Y. *ChemBioChem* **2004**, *5*, 1119−1128.

(13) Geissler, D.; Antonenko, Y. N.; Schmidt, R.; Keller, S.; Krylova, O. O.; Wiesner, B.; Bendig, J.; Pohl, P.; Hagen, V. *Angew. Chem., Int. Ed.* **2005**, *44*, 1195−1198.

(14) Hagen, V.; Dekowski, B.; Nache, V.; Schmidt, R.; Geissler, D.; Lorenz, D.; Eichhorst, J.; Keller, S.; Kaneko, H.; Benndorf, K.; Wiesner, B. *Angew. Chem., Int. Ed.* **2005**, *44*, 7887−7891.

(15) Furuta, T.; Wang, S. S.-H.; Dantzker, J. L.; Dore, T. M.; Bybee, W. J.; Callaway, E. M.; Denk, W.; Tsien, R. Y. *Proc. Natl. Acad. Sci. U.S.A.* **1999**, *96*, 1193−2000.

(16) Lin, W.; Lawrence, D. S. *J. Org. Chem.* **2002**, *67*, 2723−2726.

(17) Lu, M.; Fedoryak, O. D.; Moister, B. R.; Dore, T. M. *Org. Lett.* **2003**, *5*, 2119−2122.

(18) Montgomery, H. J.; Perdicakis, B.; Fishlock, D.; Lajoie, G. A.; Jervis, E.; Guilllemette, J. G. *Bioorg. Med. Chem*. **2002**, *10*, 1919−1927.

(19) Takaoka, K.; Tatsu, Y.; Yumoto, N.; Nakajima, T.; Shimamoto, K. *Bioorg. Med. Chem. Lett*. **2003**, *13*, 965−970.

(20) Takaoka, K.; Tatsu, Y.; Yumoto, N.; Nakajima, T.; Shimamoto, K. *Bioorg. Med. Chem.* **2004**, *12*, 3687−3694.

(21) Suzuki, A. Z.; Watanabe, T.; Kawamoto, M.; Nishiyama, K.; Yamashita, H.; Ishii, M.; Iwamura, M.; Furuta, T. *Org. Lett*. **2003**, *5*, 4867−4870.

(22) Gilbert, D.; Funk, K.; Dekowski, B.; Lechler, R.; Keller, S.; Möhrlen, F.; Frings, S.; Hagen, V. *ChemBioChem* **2007**, *8*, 89−97.

(23) Schmidt, R.; Geissler, D.; Hagen, V.; Bendig, J. *J. Phys. Chem. A* **2005**, *109*, 5000−5004.

(24) Geissler, D. Photospaltbare (Cumarin-4-yl)methyl-Ester als Phototrigger für Nucleotide, Aminosauren und Protonen. Ph.D. Dissertation, Humboldt Universtät zu Berlin, 2006; Logos Verlag Berlin: Berlin, Germany, 2007.

(25) Marquardt, D. W. *J. Soc. Ind. Appl. Math*. **1963**, *11*, 431−441.

(26) Herbrich, R.; Schmidt, R. *J. Photochem. Photobiol. A: Chem.* **2000**, *133*, 149−158.

(27) Lorimer, G. H. *Trends Biochem. Sci.* **1983**, *8*, 65−68.

(28) Lide, D. R., Ed. *Handbook of Chemistry and Physics*, 74th ed.; CRC Press: Boca Raton, FL, 1993−1994; Section 8, p 47.

(29) Kumler, W. D.; Eiler, J. J. *J. Am. Chem. Soc*. **1943**, *65*, 2355−2361.

(30) Sigel, H.; Bianchi, E. M.; Corfu, N. A.; Kinjo, Y.; Tribolet, R.; Martin, R. B. *J. Chem. Soc., Perkin Trans. 2* **2001**, 507−511.